

The Story, Properties and Applications of Bioactive Glass “1d”: From Concept to Early Clinical Trials

*Original*

The Story, Properties and Applications of Bioactive Glass “1d”: From Concept to Early Clinical Trials / Tulyaganov, D. U.; Agathopoulos, S.; Dimitriadis, K.; Fernandes, H. R.; Gabrieli, R.; Baino, F.. - In: INORGANICS. - ISSN 2304-6740. - ELETTRONICO. - 12:8(2024). [10.3390/inorganics12080224]

*Availability:*

This version is available at: 11583/2994372 since: 2024-11-13T16:29:16Z

*Publisher:*

Multidisciplinary Digital Publishing Institute (MDPI)

*Published*

DOI:10.3390/inorganics12080224

*Terms of use:*





This article is made available under terms and conditions as specified in the corresponding bibliographic description in the repository

*Publisher copyright*

(Article begins on next page)

Review

# The Story, Properties and Applications of Bioactive Glass “1d”: From Concept to Early Clinical Trials

Dilshat U. Tulyaganov <sup>1</sup>, Simeon Agathopoulos <sup>2</sup>, Konstantinos Dimitriadis <sup>3</sup>, Hugo R. Fernandes <sup>4</sup>,  
Roberta Gabrieli <sup>5</sup> and Francesco Baino <sup>5,\*</sup>

<sup>1</sup> Department of Natural-Mathematical Sciences, Turin Polytechnic University in Tashkent, Tashkent 100095, Uzbekistan; tulyaganovdilshat@gmail.com

<sup>2</sup> Department of Materials Science and Engineering, University of Ioannina, 451 10 Ioannina, Greece; sagat@uoi.gr

<sup>3</sup> Division of Dental Technology, Department of Biomedical Sciences, University of West Attica, 122 43 Athens, Greece; dimitriadiskonstantinos@hotmail.com

<sup>4</sup> Department of Materials and Ceramic Engineering, CICECO, University of Aveiro, 3810-193 Aveiro, Portugal; h.r.fernandes@ua.pt

<sup>5</sup> Department of Applied Science and Technology, Institute of Materials Physics and Engineering, Politecnico di Torino, 10129 Torino, Italy; roberta.gabrieli@polito.it

\* Correspondence: francesco.baino@polito.it

**Abstract:** Bioactive glasses in the CaO–MgO–Na<sub>2</sub>O–P<sub>2</sub>O<sub>5</sub>–SiO<sub>2</sub>–CaF<sub>2</sub> system are highly promising materials for bone and dental restorative applications. Furthermore, if thermally treated, they can crystallize into diopside–fluorapatite–wollastonite glass-ceramics (GCs), which exhibit appealing properties in terms of mechanical behaviour and overall bone-regenerative potential. In this review, we describe and critically discuss the genesis, development, properties and applications of bioactive glass “1d” and its relevant GC derivative products, which can be considered a good example of success cases in this class of SiO<sub>2</sub>/CaO-based biocompatible materials. Bioactive glass 1d can be produced by melt-quenching in the form of powder or monolithic pieces, and was also used to prepare injectable pastes and three-dimensional porous scaffolds. Over the past 15 years, it was investigated by the authors of this article in a number of in vitro, in vivo (with animals) and clinical studies, proving to be a great option for hard tissue engineering applications.

**Keywords:** bioactive glass; glass-ceramic; oxide system; diopside; fluorapatite; wollastonite; bone regeneration



**Citation:** Tulyaganov, D.U.; Agathopoulos, S.; Dimitriadis, K.; Fernandes, H.R.; Gabrieli, R.; Baino, F. The Story, Properties and Applications of Bioactive Glass “1d”: From Concept to Early Clinical Trials. *Inorganics* **2024**, *12*, 224. <https://doi.org/10.3390/inorganics12080224>

Academic Editors: Roberto Nisticò and Silvia Mostoni

Received: 29 June 2024

Revised: 7 August 2024

Accepted: 8 August 2024

Published: 17 August 2024



**Copyright:** © 2024 by the authors. Licensee MDPI, Basel, Switzerland. This article is an open access article distributed under the terms and conditions of the Creative Commons Attribution (CC BY) license (<https://creativecommons.org/licenses/by/4.0/>).

## 1. Introduction

The first bioactive glass composition, trade named as 45S5 Bioglass<sup>®</sup>, was designed by Larry Hench [1] in the early 1970s and addressed to bone replacement applications. After the invention of 45S5 glass, many other bioactive glasses have been reported for various medical applications like drug delivery [2], cancer treatment [3] or even soft tissue applications for organ repair [4]. The original 45S5 composition (45SiO<sub>2</sub>–24.5CaO–24.5Na<sub>2</sub>O–6P<sub>2</sub>O<sub>5</sub> in wt.%) is based on silica (SiO<sub>2</sub>) as the main glass-forming oxide and could create bonds with the living bone after in vivo implantations. A sequence of 11 reaction steps is involved in the bonding process of silicate bioactive glasses to living tissue [5], where the steps 1 to 5 are key for the formation of a hydroxyapatite-like layer on the surface of glasses.

Biomedical glasses are conventionally classified as “bioactive” based on these two mechanisms: (i) the formation of a calcium phosphate (hydroxyapatite-like) layer on the surface of the glass when it dissolves in a physiological environment (also in vitro in simulated body fluid (SBF)), and (ii) the release of biologically active ions during in vitro and in vivo testing. Hence, bioactive silicate glasses are both osteoconductive (mechanism (i)) and osteoinductive (mechanism (ii)). The interaction of bioactive glass surfaces with

body fluids begins with an exchange of ions that leads to an increment of the pH in the medium, resulting in the development of a SiO<sub>2</sub>-rich layer and then the growth of a CaO/P<sub>2</sub>O<sub>5</sub>-rich layer on the glass surface. This layer is further enriched with carbonates and then crystallizes to form hydroxycarbonate apatite, which mimics the mineral phase of natural bone and ultimately helps to bond with the osseous tissue [6].

The hydroxyapatite-like layer also promotes the next biological reaction stages, including cell migration, proliferation and differentiation to form new bone with good mechanical bonds to the implant surface. The hydroxyapatite layer thickness plays a major role in the bone-bonding ability of the glass as well as on the interfacial shear strength. It was reported that an interface thickness of 20 μm yields adequate shear strength and interfacial bonding [7].

Borate and borosilicate glasses are more reactive than silicate materials when in contact with body fluids or, in general, aqueous media; hence, they are less durable and can convert faster to hydroxyapatite compared to SiO<sub>2</sub>-based glasses. In principle, the bioactivity mechanism is very similar except for the formation of a borate-rich gel layer, analogous to the silica gel layer in silicate systems. The apatite-formation rate can be controlled by changing the glass composition, thus varying the reaction time from hours to months [8].

Phosphate glasses have also been proposed for bone tissue engineering applications; their tendency to rapidly dissolve in aqueous media depending on the composition—and, especially, on the metal oxide content—has pushed their use towards advanced therapies mediated by controlled ions release [9].

When high-strength and/or load-bearing applications are major goals, the controlled crystallization of silicate glasses yielding bioactive glass-ceramic (GC) materials is an attractive option. For example, the commercial apatite/wollastonite (A–W)-containing Cerabone (SiO<sub>2</sub>-CaO-MgO-P<sub>2</sub>O<sub>5</sub>-F parent system) has been produced by controlled heat treatment, obtaining 38 wt.% apatite, 34 wt.% of wollastonite and 38 wt.% of residual glass phase, and used as a coating for titanium alloys, artificial vertebrae and bone fillers [10,11]. The bending strength of these A–W glass-ceramics (GCs) is typically higher than that of human cortical bone (160 MPa), but the fracture toughness is three times lower (6 MPa m<sup>1/2</sup>) [12]. Interestingly, it was observed that hydroxyapatite can form on the surface of these GCs even if the silica gel on the surface is absent, as the apatite and wollastonite crystals act as sites for direct nucleation of calcium phosphate phases [13].

Other common examples of bioactive GCs include A–W Ceravital and diopside-containing products, such as apatite–diopside (AD), wollastonite–diopside (WD) and diopside–combeite (DC) GCs. Ceravital (SiO<sub>2</sub>-CaO-MgO-Na<sub>2</sub>O-K<sub>2</sub>O-P<sub>2</sub>O<sub>5</sub> parent system) [14] has an analogous bioactivity mechanism to Hench's 45S5 Bioglass<sup>®</sup>, along with good mechanical properties and better stability in the long term. After the implantation of Ceravital material, an initial degradation of the surface caused by ionic exchange was observed, followed by the formation of reaction layers that protect the implant from further chemical attacks.

The phase in common for the other GC types mentioned above is diopside, which is very appealing for biomedical applications due to its attractive mechanical performance. For example, diopside was combined with hydroxyapatite in order to increase the fracture resistance of the latter [15]. In this case, the fracture strength of the AD bioceramic was found to be 2–3 times higher compared to hydroxyapatite alone; moreover, the material was non-toxic to the body cells and promoted bone regeneration.

In wollastonite–diopside GCs, wollastonite and diopside phases form when the parent glass is thermally treated above 900 °C. Both wollastonite and diopside have good mechanical properties and the latter has a slower dissolution rate upon contact with body fluids. These bioactive GCs have been used in bulk, granular and porous forms for bone graft applications [16].

DC GCs have also been proposed for bone-contact applications; it is worth mentioning that combeite is a highly biocompatible phase, which is typically found in sintered 45S5 Bioglass<sup>®</sup> treated above 550 °C, too [17].

Therefore, all these studies witnessed that diopside was an attractive crystalline phase to have inside GC biomaterials. These results pushed scientists to design new glass-derived formulations that could originate GC products with superior biological and mechanical properties, of which the “1d” composition is a valuable example.

## 2. The Genesis of the 1d Composition

The glass composition 1d (Table 1) was designed so that, upon thermal devitrification, a final GC material containing diopside, fluorapatite and wollastonite could be obtained with high mechanical strength and excellent bioactive properties [18].

**Table 1.** Chemical composition of 1d glass and some of its derivatives (in wt.%) [18–20].

Composition	SiO <sub>2</sub>	CaO	MgO	P <sub>2</sub> O <sub>5</sub>	Na <sub>2</sub> O	K <sub>2</sub> O	CaF <sub>2</sub>
<i>Parent glass composition</i>							
<b>1d</b>	<b>46.1</b>	<b>28.7</b>	<b>8.8</b>	<b>6.2</b>	<b>4.5</b>	<b>0</b>	<b>5.7</b>
1d-a	41.8	32.85	8.85	6.24	4.54	0	5.72
1d-b	37.51	37.07	8.88	6.26	4.55	0	5.73
1e	43.5	30.4	8.8	7.2	4.5	0	5.6
1e-a	43.09	30.13	8.67	9.17	4.44	0	4.47
1e-b	42.71	29.85	8.59	11.1	4.41	0	3.33
1e-c	42.33	29.59	8.52	13.00	4.37	0	2.19
<i>K<sub>2</sub>O for Na<sub>2</sub>O substitution</i>							
<b>1d-k</b>	<b>45.0</b>	<b>28.0</b>	<b>8.60</b>	<b>6.1</b>	<b>0</b>	<b>6.7</b>	<b>5.6</b>
1e-k	42.5	29.7	8.5	7.1	0	6.7	5.5
<i>MgO for CaO partial substitution</i>							
<b>1d-m</b>	<b>46.6</b>	<b>24.8</b>	<b>11.9</b>	<b>6.3</b>	<b>4.6</b>	<b>0</b>	<b>5.8</b>
1e-m	44.00	26.7	11.8	7.3	4.5	0	5.7

The 1d composition relies on the primary crystallization field of pseudowollastonite in the CaO–MgO–SiO<sub>2</sub> ternary system, in which P<sub>2</sub>O<sub>5</sub>, Na<sub>2</sub>O and CaF<sub>2</sub> were added. Following a melt-quenching route, 1d products can be obtained in an amorphous form (glass) but the development of the three crystalline phases mentioned above can be induced by applying a proper thermal treatment.

The 1d glass was the most promising member of a family of compositions, which were originally designed and studied by a multidisciplinary international research team and resulted in numerous publications since 2006; other sister formulations include 1e glass—having the same components as 1d in different amounts [18–20]—and 1b glass [21,22], also containing B<sub>2</sub>O<sub>3</sub> as an additional oxide.

Similarly, other glasses based on the 1d and 1e compositions have been created by replacing the components and changing the ratio of percentages by weight, such as the following:

- 1d-a and 1d-b: in which the CaO/SiO<sub>2</sub> ratio has been progressively increased [18] (Table 1);
- 1e-a, 1e-b, 1e-c: in which the P<sub>2</sub>O<sub>5</sub>/CaF<sub>2</sub> ratio has been progressively increased [18] (Table 1);
- 1d-k, 1e-k: where Na<sub>2</sub>O was replaced with K<sub>2</sub>O [19,20] (Table 1);
- 1d-m, 1e-m: where CaO was partially replaced with MgO [19,20] (Table 1).

## 3. Material Preparation and Basic Properties

The 1d glass is typically synthesized by following a melt-quenching route; several publications can be found in the literature where the basic preparative process has been applied with some modifications, as summarized in Table 2, from the reagent powders to frit production. Examples of 1d glass frit and glass powders after milling are given in Figure 1.

**Table 2.** Processes to obtain 1d glass powder from precursors powders.

Article	Powders	Batch and Milling	Heat Treatment	Frits and Glass Powders
I. Kansal et al. [18]	SiO <sub>2</sub> (purity > 99.5%), CaCO <sub>3</sub> (>99.5%), MgCO <sub>3</sub> (>99%), Na <sub>2</sub> CO <sub>3</sub> (>99%), CaF <sub>2</sub> (>99.9%), NH <sub>4</sub> H <sub>2</sub> PO <sub>4</sub> (>99%)	Homogenous mixture of precursors of about 100 g obtained by ball milling.	Pre-heating at 900 °C for 1 h for calcination. Melting in Pt crucible at 1450–1550 °C for 1 h.	Frits are obtained by quenching of melted glass in water. Frits are dried and then milled in agate mill. Powders are sieved to obtain a mean particle size of about 10 µm.
D. U. Tulyaganov et al. [22]	SiO <sub>2</sub> (purity>99.5%), CaCO <sub>3</sub> (>99.5%), 4MgCO <sub>3</sub> ·Mg(OH) <sub>2</sub> ·5H <sub>2</sub> O (>99%), Na <sub>2</sub> CO <sub>3</sub> (>99%), CaF <sub>2</sub> (>99%), NH <sub>4</sub> H <sub>2</sub> PO <sub>4</sub> (>99%)	Homogenous mixture of precursors of about 100 g obtained by ball milling.	Pre-heating at 1000 °C for 1 h for decarbonization. Melting in Pt crucible at 1400 °C for 1 h.	Frits are obtained by quenching of melted glass in water. Frits are dried and then milled in a porcelain mill. Powders are sieved to obtain a mean particle size of 11–14 µm.
S. I. Schmitz et al. [23]	SiO <sub>2</sub> (purity > 99.5%), CaCO <sub>3</sub> (>99.5%), 4MgCO <sub>3</sub> ·Mg(OH) <sub>2</sub> ·5H <sub>2</sub> O (>99%), Na <sub>2</sub> CO <sub>3</sub> (>99%), CaF <sub>2</sub> (>99%), NH <sub>4</sub> H <sub>2</sub> PO <sub>4</sub> (>99%)	Homogenous mixture of precursors.	Pre-heating at 1000 °C for 1 h for decarbonization. Melting in Pt-crucible at 1400 °C for 1 h.	Frits are obtained by quenching of melted glass in deionized water. Frits are dried and then milled in a planetary mill. Powders are sieved to obtain a final particle size <32 µm.
D. U. Tulyaganov et al. [24]	SiO <sub>2</sub> (purity > 99.5%), CaCO <sub>3</sub> (>99.5%), MgCO <sub>3</sub> (>99%), Na <sub>2</sub> CO <sub>3</sub> (>99%), CaF <sub>2</sub> (>99%), NH <sub>4</sub> H <sub>2</sub> PO <sub>4</sub> (>99%)	Homogenous mixture of precursors.	Pre-heating at 1000 °C for 1 h for decarbonization. Melting in Pt crucible at 1400 °C for 1 h.	Frits are obtained by quenching of melted glass in water. Frites are dried and then milled. Powders are sieved to obtain a mean particle size of 10–15 µm.
K. Dimitriadis et al. [20]	SiO <sub>2</sub> (purity > 99.5%), CaCO <sub>3</sub> (>99.5%), Mg(NO <sub>3</sub> ) <sub>2</sub> ·6H <sub>2</sub> O (>99%), Na <sub>2</sub> CO <sub>3</sub> (>99%), CaF <sub>2</sub> (>99%), (NH <sub>4</sub> ) <sub>2</sub> HPO <sub>4</sub> (>99%)	Homogenous mixture of precursors of about 100 g.	Pre-heating at 900 °C for 1 h for decarbonization. Melting in Pt crucible at 1400 °C for 1 h.	Frits are obtained by quenching of melted glass in water. Frits are dried and then milled in a planetary mill. Powders are sieved to obtain a final particle size <32 µm.
F. Baino et al. [25]	SiO <sub>2</sub> (purity > 99.5%), CaCO <sub>3</sub> (>99.5%), MgCO <sub>3</sub> (>99%), Na <sub>2</sub> CO <sub>3</sub> (>99%), CaF <sub>2</sub> (>99.9%), NH <sub>4</sub> H <sub>2</sub> PO <sub>4</sub> (>99%)	Homogenous mixture of precursors of about 100 g by ball milling.	Pre-heating at 850 °C for 1 h in an Al <sub>2</sub> O <sub>3</sub> at heating rate of 2.5 °C/min. Melting in Pt crucible at 1420 °C for 1 h.	Frits are obtained by quenching of melted glass in water. Frits are dried and then milled in a planetary mill. Powders are sieved to obtain a final particle size <56 µm.
K. Dimitriadis et al. [19]	SiO <sub>2</sub> (purity > 99.8%), CaCO <sub>3</sub> (>99%), Mg(NO <sub>3</sub> ) <sub>2</sub> ·6H <sub>2</sub> O (>99%), Na <sub>2</sub> CO <sub>3</sub> (>99.6%), CaF <sub>2</sub> (>99%), (NH <sub>4</sub> ) <sub>2</sub> HPO <sub>4</sub> (>99%)	Homogenous mixture of precursors of about 100 g by ball milling.	Pre-heating at 900 °C for 1 h in an Al <sub>2</sub> O <sub>3</sub> crucible at heating rate of 1.5 °C/min. Melting in Pt crucible at 1400 °C for 1 h.	Frits are obtained by rapid pouring of melted glass in water. Frits are dried and then milled in a planetary ball-mill at 400 rpm for 45 min in a YSZ milling jar. Powders are sieved to obtain a final particle size <32 µm.

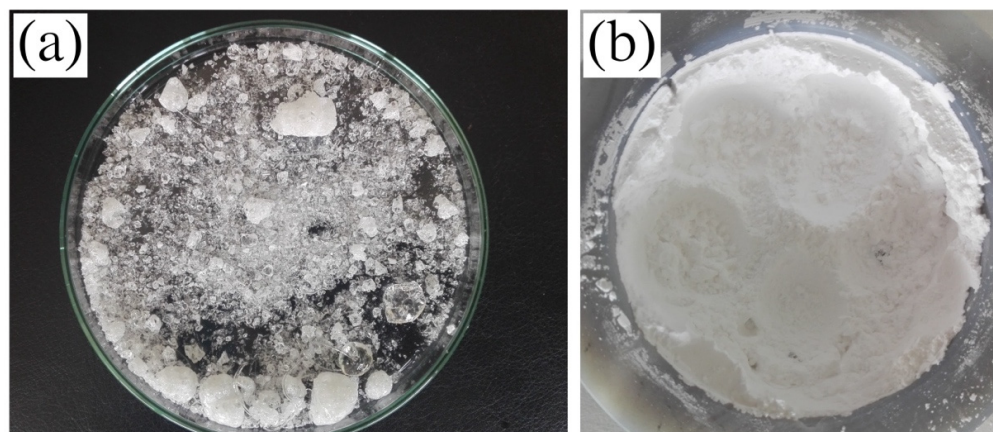


**Figure 1.** Example of (a) 1d glass frit, (b) glass powders after ball milling.

The density of 1d glass was reported to be  $2.57 \pm 0.13 \text{ g/cm}^3$ , the characteristic temperatures, i.e., glass transition ( $T_g$ ), onset of crystallization ( $T_c$ ) and peak of crystallization ( $T_p$ ), were assessed in various publications (also by using different experimental methods) and are collected in Table 3.

**Table 3.** Characteristic temperatures of 1d glass: glass transition ( $T_g$ ), onset of crystallization ( $T_c$ ) and peak of crystallization ( $T_p$ ).

Article	$T_g$ (°C)	$T_c$ (°C)	$T_p$ (°C)
K. Dimitriadis et al. [19]	$649 \pm 9$	$783 \pm 2$	$815 \pm 13$
F. Baino et al. [25]	640	785	830
K. Dimitriadis et al. [20]	$655 \pm 5$	$783 \pm 2$	$845 \pm 13$
D. U. Tulyaganov et al. [24]	$607 \pm 7$	-	$815 \pm 13$
D. U. Tulyaganov et al. [22]	$590 \pm 10$	-	-

#### 4. Crystalline Phases and Mechanical Properties

Powders of 1d glass have been used as-is, even in clinical trials (as discussed later [26]), or as starting materials to fabricate other products, such as 3D porous scaffolds for bone tissue engineering. To obtain these 1d-derived implants, a thermal treatment is necessary to consolidate and join the glass particles together, during which sinter-crystallization may take place. In other words, the formation of crystalline phases is promoted upon heating, leading to the material's transformation from purely amorphous to a GC state with the development of wollastonite, fluorapatite and diopside. Figure 2 shows the microstructure of 1d-derived GCs, in which the part formed by prisms corresponds to diopside, wollastonite crystals have a needle-like shape, and flakes refer to fluorapatite [19].

Table 4 illustrates the influence of heat-treatment temperatures on the mechanical properties of various 1d-derived GCs. It is known that crystallization yields an improvement in the mechanical properties of GCs compared to parent glass; accordingly, the highest increments of flexural strength, elastic modulus, hardness and fracture toughness, were achieved in the GC produced by heat treatment at  $850 \text{ }^\circ\text{C}$ , i.e., a temperature close to  $T_p$  (see Table 3). It was also determined that the brittleness indexes of the produced 1d- and 1e-derived GCs ranged between 3.6 and 3.7 and 3.3 and  $3.5 \mu\text{m}^{-0.5}$ , respectively. Qualitatively, machinability reflects the easiness of a material to be cut, and it can be quantified by the magnitude of brittleness [27]. The 1d- and 1e-derived GCs exhibited a brittleness index higher than  $3 \mu\text{m}^{-0.5}$  [28], thus being in the preferred range as the brittleness index for glasses and ceramics typically ranges from 3 to  $9 \mu\text{m}^{-0.5}$  [27]. This discovery holds significance for dental materials production, as these materials are often shaped using specialized cutting tools. Therefore, the aforementioned brittleness index values suggest a reduced risk of fractures or cracks occurring during these processes especially for the

1d-derived GC, since it shows a higher value on the brittleness index compared to the 1e-derived GC [28].

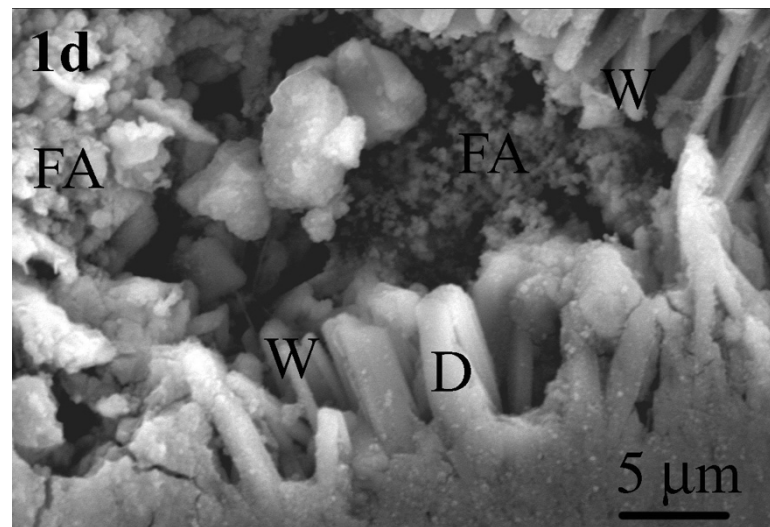


**Figure 2.** Typical microstructure of 1d-derived GCs produced by heat treatment at 850 °C for 1 h. Observation was performed after etching the polished surface with 2% HF solution (D: diopside; FA: fluorapatite; W: wollastonite).

**Table 4.** Mechanical properties of different 1d-derived GCs compared to other GCs containing diopside, wollastonite and fluorapatite as crystalline phases.

Materials	Heat Treatment (°C)	Flexural Strength ( $\sigma$ , MPa)	Elastic Modulus (E, GPa)	Vickers Microhardness (HV, GPa)	Fracture Toughness ( $K_{IC}$ , MPa · m <sup>0.5</sup> )
1d-derived GCs [28]	800	119 ± 10	24 ± 6	6.0 ± 0.4	1.6 ± 0.1
	850	171 ± 11	27 ± 5	6.1 ± 0.5	1.7 ± 0.1
	900	141 ± 6	22 ± 4	5.2 ± 0.7	1.4 ± 0.1
GCs containing diopside and fluorapatite [29]	850	120–195	-	-	-
GCs containing wollastonite and quartz [30]	900–1000	98 ± 6	-	5.9–6.7	-
GCs containing wollastonite, hydroxyapatite and fluorite [31,32]	700–1000	-	89–100	-	4.6–5.6
GCs containing wollastonite [33]	3100 (flame-spraying)	-	37–56	2.6–5.4	-
GCs containing wollastonite and diopside [33]	3100 (flame-spraying)	-	62–77	2.2–6.5	-

The main characteristics of these three crystalline phases contributing to mechanical properties of GCs (Table 4) are described in the following sections.

#### 4.1. Fluorapatite

Fluorapatite is a mineral that is part of the apatite family with the chemical formula  $\text{Ca}_{10}(\text{PO}_4)_6\text{F}_2$ . It is a double salt resulting from the bond between calcium phosphate and calcium fluoride. It is a highly biocompatible material and fits well with bone repair

applications. In fact, it is present in nature and is part, for example, of the mineralized phase of bones and teeth in mammals [34].

Moreover, having the fluoride ion instead of the hydroxyl ion, fluorapatite exhibits peculiar characteristics that differentiate it from hydroxyapatite; in fact, the former is much less soluble in an acidic environment, such as that of the human mouth, compared to hydroxyapatite. However, despite few differences in some physicochemical properties, the structure of both calcium phosphates is substantially the same. If in hydroxyapatite there are calcium phosphate tetrahedra arranged around hydroxyl ion columns, in fluorapatite there are tetrahedra which develop around fluoride columns (Figure 3).

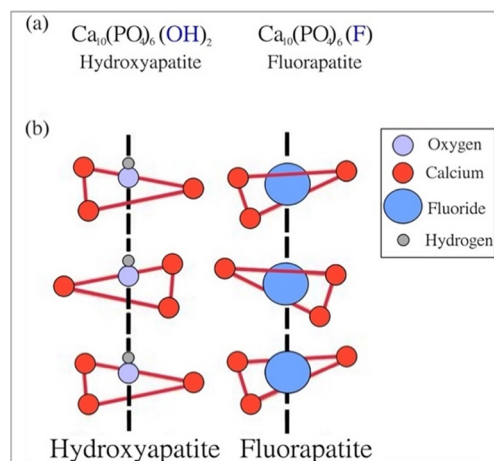


**Figure 3.** Similarities between fluorapatite and hydroxyapatite: (a) chemical formulas and (b) chemical structures. Reproduced from [35] with permission.

The crystalline structure of fluorapatite, characterised by flake-like crystals, can be visualized in the SEM image displayed in Figure 4. These morphological observations are also in agreement with theoretical expectations (see Figure 3).

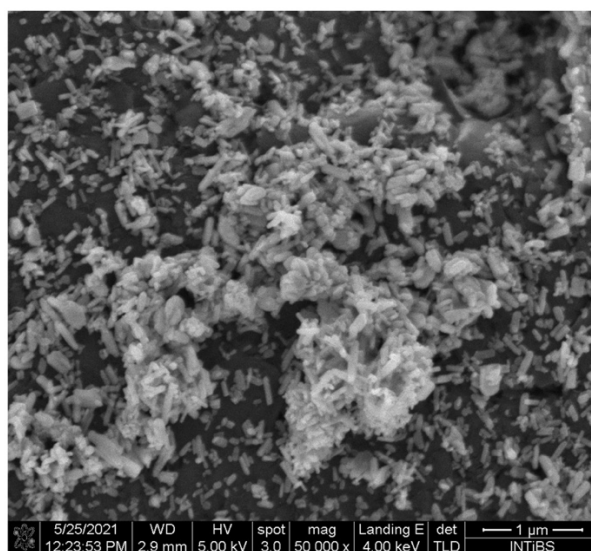


**Figure 4.** SEM image of fluorapatite. Reproduced from [36] under CC license.

#### 4.2. Wollastonite

Wollastonite is a mineral with interesting characteristics for biomedical applications, including biocompatibility, biodegradability, thermal stability/low thermal expansion, low thermal conductivity and high mechanical properties [37,38]. Given these appealing properties, in the early 1980s, Kokubo et al. [39] first produced a bioactive GC containing



both apatite and wollastonite. This new biomaterial belonged to a more complicated system than that invented by Hench one decade earlier (45S5 Bioglass<sup>®</sup>) [40]. This GC contained apatite (38%), wollastonite (24%) and residual amorphous phase (38%) [39] and has been since marketed under the commercial name of Cerabone<sup>®</sup>.

Wollastonite is a simple calcium silicate with the chemical formula  $\text{CaSiO}_3$ ; alternatively, it can be seen as a mixture of silica ( $\text{SiO}_2$ ) and lime ( $\text{CaO}$ ) having a theoretical percentage of 51.7% and 48.3%, respectively [37]. Due to its crystal structure (Figure 5), wollastonite belongs to the class of minerals known as pyroxenoids. It was reported that pyroxenoid chains are more kinked and have a great repeat distance [37].

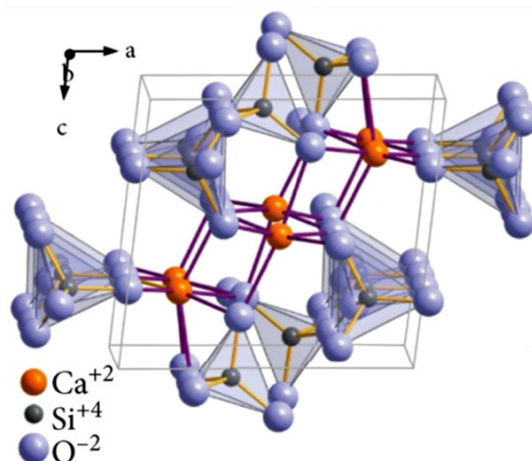


**Figure 5.** Crystalline structure of wollastonite. Reproduced from [37] under CC license.

Two polymorphs of wollastonite,  $\alpha$ -phase and  $\beta$ -phase, potentially exist in nature: the  $\beta$ -phase is the stable state at low temperatures, while the  $\alpha$ -phase is found above 1125 °C [41]. Therefore, wollastonite used in biomedical implants is typically the  $\beta$  type and has been proposed as filler in composite fabrication in orthopaedics as well as for dental restoration [37]. The needle-like shape of  $\beta$ - $\text{CaSiO}_3$  crystals is shown in Figure 6.

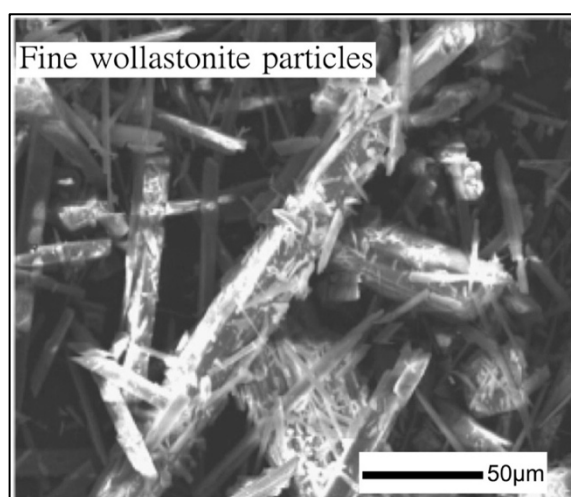


**Figure 6.** SEM image of wollastonite. Reproduced from [42] with permission.

#### 4.3. Diopside

Diopside ( $\text{CaMgSi}_2\text{O}_6$ ) is a prismatic monoclinic mineral, but it is not always possible to have this structure; on the contrary, it is easier to find granular and globular structures [43]. The crystalline structure of diopside is very similar to pyroxene, as displayed in Figure 7.

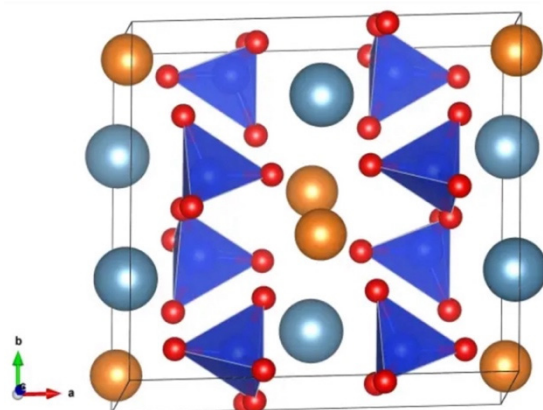


**Figure 7.** Crystalline structure of diopside found by Warren and Bragg: light blue spheres are calcium atoms, orange spheres are magnesium atoms, each tetrahedron consists of 1 silicon atom and 4 oxygen atoms (red spheres) [44].

Diopside was found to exhibit superior mechanical properties compared to other commonly used bioceramics. For example, it presents a bending strength of 300 MPa and a fracture toughness of  $3.5 \text{ MPa m}^{1/2}$ , which are higher with respect to wollastonite-containing ceramics with similar densities and exceed those of hydroxyapatite by 2–3 times [45].

Diopside was also found to be able to bond with living bone tissue. In this regard, Nonami and Tsutsumi [15] conducted a high-resolution electron microscopy study revealing the continuity between diopside implants and bone tissue in monkeys and rabbits, which was possible due to growth of new tissue at the interface. The same authors also reported that diopside had a much longer degradation time than hydroxyapatite, which was not optimal for bone regeneration; however, this can be useful in those cases where more chemical stability is required or for dental roots.

## 5. Comparison between 1d Formulation and 45S5 Bioglass<sup>®</sup>

As previously stated, bioactive glasses in the CaO-MgO-SiO<sub>2</sub> ternary system as well as their relevant GC derivatives can indeed be designed for potential use in bone repair, but it is necessary to compare the major characteristics of these new materials with a “gold standard” reference, such as 45S5 Bioglass<sup>®</sup>. A series of studies were carried out for this specific purpose, as discussed in the next sections.

### 5.1. Chemical Composition

Table 5 highlights the quantitative differences in the composition of 1d and 45S5 glasses, in terms of amount of ingredients.

**Table 5.** Nominal compositions of 1d glass and 45S5 Bioglass<sup>®</sup>.

Glasses	SiO <sub>2</sub>	CaO	MgO	P <sub>2</sub> O <sub>5</sub>	CaF <sub>2</sub>	Na <sub>2</sub> O
1d glass (wt.%)	46.1	28.7	8.8	6.2	5.7	4.5
45S5 Bioglass <sup>®</sup> (wt.%)	45	24.5	-	6	-	24.5

The two bioactive glasses have a similar number of former oxides (SiO<sub>2</sub> and P<sub>2</sub>O<sub>5</sub>); the content of CaO is higher for 1d glass.

The main differences between the two bioactive glasses can be summarized in two points:

1. The content of Na<sub>2</sub>O in 45S5 is more than five times greater when compared to 1d;
2. The 1d glass contains additional MgO and CaF<sub>2</sub>, which are not present in the case of the 45S5 Bioglass<sup>®</sup>.

The presence of magnesium within the glass composition is useful because Mg<sup>2+</sup> ions are naturally contained in bone tissue and play an active role in human bone metabolism.

Magnesium ions promote cell adhesion, proliferation and differentiation of osteoblasts [23]. Moreover, Dietrich et al. [46] noted that having an amount of MgO in the glass composition between 0.4 and 1.2 wt.% accelerates glass dissolution, consistent with its role as network modifier.

Instead, the partial substitution of Na<sub>2</sub>O with CaF<sub>2</sub> has the effect of decreasing the pH in the surrounding solution during in vitro tests, as well as the melting and glass transition temperatures of the glass; furthermore, a change in cell response was also reported [23]. In this regard, in vitro results with mesenchymal stem cells suggested an advantage of 1d glass concerning cell viability and proliferation. On the other hand, the ions released from 45S5 material appeared to have a stronger osteoinductive effect, whereas no clear superiority of either of the bioactive glasses was observed upon direct cell–glass contact [23]. Further tests are necessary to elucidate these issues, also considering that different experimental conditions could have played a role (e.g., the particle sizes used in that study: <32 μm for 1d and <56 μm for 45S5 glass).

### 5.2. Advanced Microstructural Analysis (Q<sup>n</sup> Units)

Figure 8 shows the Fourier-transformed infra-red (FTIR) spectra of 1d and 45S5 glasses acquired in the wavenumber range of 300 to 1300 cm<sup>-1</sup>. In order to study the distribution of Q<sup>n</sup> (i.e., the degree of polymerization of the structure inside the glass, where n indicates the number of bridging oxygens), Kansal et al. [18] focused on the range within 900–1100 cm<sup>-1</sup>, which corresponds to SiO<sub>4</sub> with a different number of bridging oxygens.

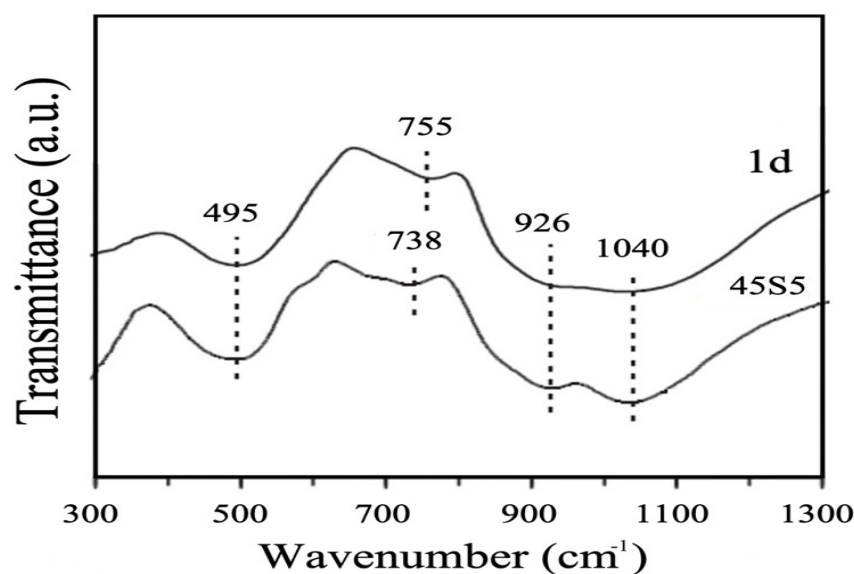


**Figure 8.** FTIR spectra of bioactive glasses 1d and 45S5. Reproduced from [18] with permission.

There were two interesting bands in this range, around 1040 cm<sup>-1</sup>, which indicate the presence of silicate Q<sup>3</sup> units, and around 930 cm<sup>-1</sup>, which indicate the polymerization of silicate Q<sup>2</sup> units along with some Q<sup>1</sup> units. As reported by Tilocca [47], the highest bioactivity of phosphosilicate glasses can be expected if Q<sup>n</sup> units are dominated by chains of Q<sup>2</sup> metasilicates, which are sporadically cross-linked through Q<sup>3</sup> units, whereas the chains are terminated by Q<sup>1</sup> units. The structures of 1d and 45S5 glasses are similar since the predominant units are Q<sup>2</sup> and Q<sup>3</sup> for both materials; hence, a high apatite-forming ability is expected. The number of non-bridging oxygens per each tetrahedron was calculated for both 45S5 and 1d glasses, resulting to be 1.99 and 1.88, respectively. These values suggest that 1d glass has a more cross-linked structure than 45S5 Bioglass<sup>®</sup> because, although predominantly containing Q<sup>2</sup> units, it has a larger fraction of Q<sup>3</sup> units compared to the other glass [21].

### 5.3. pH In Vitro

Tulyaganov et al. [26] conducted immersion studies in SBF to evaluate the effect of 1d and 45S5 glasses on the pH of the solution. Over the first 300 h, there was a noticeable rise in pH in the case of 45S5 Bioglass<sup>®</sup> from 7.10 to about 7.75. This increase was due to the ion exchange mechanism already proposed by Hench [5,6,10,13] and explained above. On the contrary, a more moderate increment in pH was observed in the experiment with 1d glass, which was associated with the presence of fluoride ions that were exchanged with OH<sup>−</sup> ions from the SBF (from the dissociation of water into H<sup>+</sup> and OH<sup>−</sup>), eventually leading to a pH decrease. This was also consistent with other findings about fluoride-containing bioactive glasses [48].

Having a moderately alkaline pH around the implant (up to 7.8–8.0) carries some advantages, such as the accelerated formation of the apatite layer on the glass surface and the stimulation of the viability of osteoblasts; however, if the pH value is too high, damage to tissues and bone cells may occur as well as the inhibition of endothelial cell proliferation [26].

### 5.4. Mass Loss

Because of the different chemical compositions, there is also a different dissolution rate of 1d and 45S5 glasses in testing solutions. Tulyaganov et al. [26] reported that the mass loss was much higher in the case of Hench's glass (3.7 wt.%) when compared to the 1d composition (2 wt.%) after soaking for 120 h in Tris-HCl. For completeness, it was also reported that the pH value inside this solution increased more significantly after immersion of 45S5 when compared to 1d glass (9.7 versus 8.1, from a starting value of 7.2).

### 5.5. In Vitro Bioactivity

XRD patterns of the two different bioactive glass compositions, before and after immersion in SBF for different time frames, are reported in Figure 9.

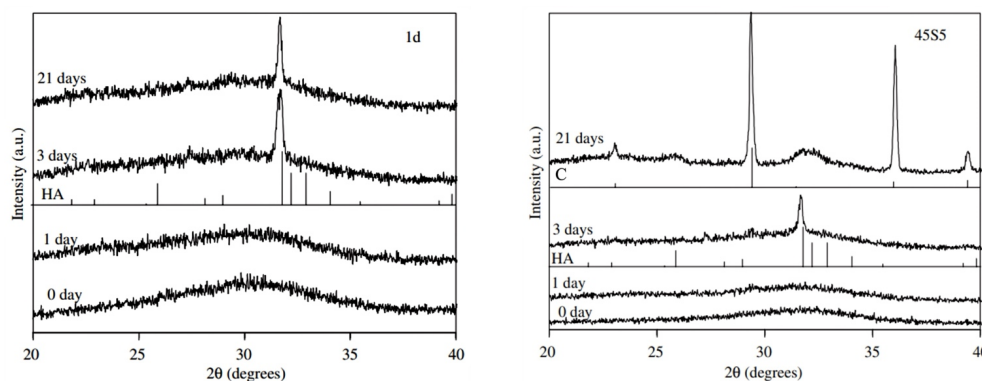


**Figure 9.** XRD patterns of 1d glass (**left**) and 45S5 Bioglass<sup>®</sup> (**right**). HA = hydroxyapatite; C = calcite. Reproduced from [26] with permission.

The common feature in both as-produced materials is the presence of the amorphous halo in the range of 28 to 35°, which is typical of silicate glasses. No detectable modifications can be seen after 1 day of immersion in SBF but, after 3 days, the characteristic peaks of hydroxyapatite—especially the main reflection (211) at ~32°—begin to develop. At this time point, the (211) diffraction peak of hydroxyapatite was sharper in the case of the 1d glass compared to 45S5 [26].

The results after 21 days show a different behaviour for the two bioactive glasses; in fact, while only hydroxyapatite was found to grow on the 1d surface, in the case of 45S5 glass, there were some peaks related to calcium carbonate (calcite), too. The coexistence of apatite and calcite was reported to occur in some in vitro studies, which may depend on multiple factors (e.g., glass particle size, volume of solution used, glass composition) not fully elucidated yet, as comprehensively discussed elsewhere [49].

### 5.6. Direct and Indirect Cell Culture

Schmitz et al. [23] performed an experiment to investigate the biological responses elicited by 45S5 and 1d glasses in two different cell-culture settings with a focus on cell proliferation, viability and osteogenic differentiation:

- (a) Indirect culture: the bioactive glasses were immersed in a solution for 24 h at body temperature and shaken to promote the release of ionic dissolution products. At the end of this first phase, the glasses were removed, and the solution was filtered and used as a culture medium for mesenchymal stem cells (MSCs). This setting is used to verify the effects of the ions released.
- (b) Direct culture: the bioactive glasses removed from the solution in the point (a) were placed in direct contact with MSCs.

The use of both settings was very useful to describe in detail both the action of the ions that were released by the bioactive glasses through the indirect culture setting and the reactions that take place once the physical contact of the materials with the cells occurs through the direct culture setting.

The major results from the two different settings can be summarized as follows:

- Indirect culture setting: 45S5 glass elicited a better osteogenic action compared to 1d glass. This behaviour was because, in the former case, there was a higher concentration of P and Si ions in the cell culture medium having osteostimulatory effects. In fact, phosphorus stimulates osteogenic differentiation and bone mineralization [50], and Si ions also activate gene families in bone cells, ultimately promoting osteogenic differentiation [51].
- Direct culture setting: there was a reversal in the trend compared to the indirect culture setting. In fact, the osteogenic action was no longer so different between the two bioactive glasses, although the expression of the specific protein OCN (marker of osteogenic differentiation) was greater in the 1d cultures. The concentration of magnesium, which was released by the 1d glass, in the first 24 h was one tenth of that detected after a week, and the concentration of Ca increased over time in the medium. This progressive, increasing release of beneficial ions is important as magnesium ions have the ability to increase cell viability [52], and calcium ions improve cell viability and proliferation [53]. These promising in vitro results on 1d glass were corroborated by in vivo tests.

The obtained results demonstrated an advantage of 1d glass in regard to cell viability and proliferation. Owing to its good osteogenic potential compared to the benchmark 45S5 glass and its higher biocompatibility, 1d glass was proposed to be an interesting alternative to 45S5 glass for bone tissue engineering applications [23].

### 5.7. Antibacterial Properties

The antibacterial properties of some experimental compositions based on 1d glass were tested against *Escherichia coli* (*E. coli*) [54]. Silver from 0.035 M, 0.077 M, 0.150 M and 0.220 M AgNO<sub>3</sub> aqueous solutions have been incorporated into the surface of 1d bioactive glass through the ion exchange approach assisted with ultrasonic treatment. Antibacterial tests showed that the silver-containing glasses inhibited the growth of *E. coli*, which exhibited a rapid decrease in its viability, reaching the limit of detection after a maximum of 2 h. Parent 1d glass induced a slight decrease in bacterial number after one hour compared with the bacterial inoculum. However, after two hours of incubation at 37 °C, the number of bacteria increased again, being comparable to the inoculum. It was observed that, according to the mid IR spectra, the structure of silver-modified glasses was similar to that of the parent 1d glass, which indicates that the treatment performed did not significantly alter the structure of the glass network and, thus, was not expected to interfere with its bioactivity mechanisms.

## 6. In Vivo Experiments and Clinical Trials

Tulyaganov et al. [26] studied the effects of bioactive glass 1d on both animals and human patients. In the first set of experiments, 1d glass particles were inserted directly into osseous defects produced in rabbit femora after being properly sterilized. Reactions in rabbits were monitored at different time points, i.e., 1 week, 2 weeks, 1 month, 2 months, 3 months, 4 months and 6 months (Figure 10).

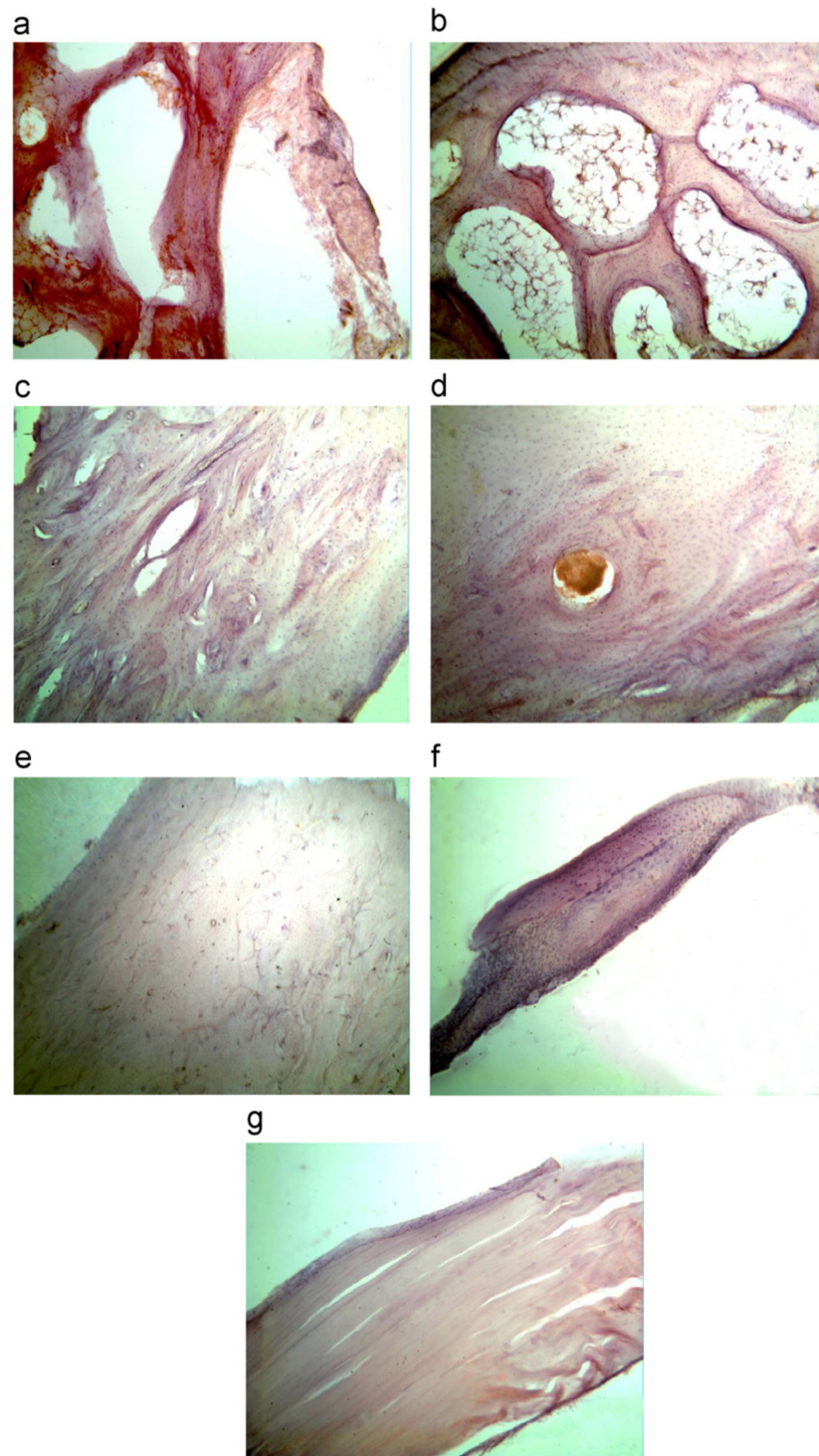


**Figure 10.** Histopathological sections of the bone in cortical area of bone (magnification 400×) after implantation for different periods: (a) 1 week; (b) 2 weeks; (c) 1 month; (d) 2 months; (e) 3 months; (f) 4 months; and (g) 6 months. Reproduced from [26] with permission.

Since the first week, the presence of low inflammatory infiltrate and an increase in the thickness of blood vessels was observed. From the first month onwards, the formation of new bone began, starting from the outside and spreading inwards. As the months passed, the bone trabeculae became thicker and thicker, and the implanted material was progressively embedded inside the newly formed bone. After 6 months, the surgically created cavities were completely filled with regenerated bone, which was mature and homogeneous. Overall, 1d glass powders were fully compatible with the surrounding tissues without eliciting any significant adverse reaction throughout the experiment duration.

The same 1d glass particulate was clinically tested over 8 months to treat jawbone defects in human patients mainly after a cystectomy operation. The test was conducted in 45 volunteers (21 males and 24 females) aged between 19 and 60. Patients were examined before and after surgery at 2 weeks, 2 months and 6 months. In this study, glass particles were inserted where there was a defect in the alveolar bone in order to avoid the progressive loss of bone over time (resorption) and assure the stability of the patient's teeth. These early clinical trials showed that the glass formed a cohesive mass with the patient's blood, thus demonstrating a homeostatic effect. Figure 11 shows that new, regenerated bone was formed after 2 months where there was the empty space of a jawbone defect before surgery. Similar results were found in all patients and, thus, these early clinical trials support the suitability of 1d glass for the conventional treatment of bone defects (highly biocompatible and bioactive filler). Figure 12 shows two other radiographs of the patient showing that after a cystectomy operation, the lesions were filled up with newly formed cancellous bone. However, in order to gain regulatory approval and consider this bioactive glass for routine surgery, it will be necessary to increase the number of patients during a further phase of clinical trials.

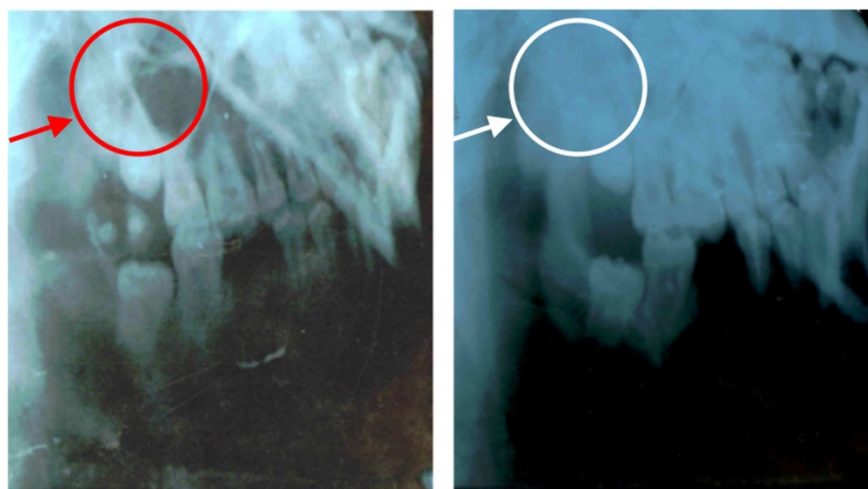


**Figure 11.** Radiographic images of jawbone defects before ((left) side) and after surgical intervention (2 months of follow-up) with implantation of 1d glass particulates ((right) side). Reproduced from [26] with permission.

In an attempt to avoid undesired losses of glass particulates during the grafting procedure and to further improve the handling properties, composites based on bioactive glass 1d and organic carriers, i.e., glycerol and polyethylene glycol (PEG), were synthesized [55]. Homogeneous mixtures were obtained that could be handled as mouldable pastes, demonstrating cohesive injectability. All pastes exhibited high apatite-forming rates after immersion in SBF, consistent with the *in vitro* bioactivity of 1d particles. The potential suitability of these materials for osteostimulatory bone healing was recently confirmed *in vivo* through implantation experiments in rabbit femoral defects [24].

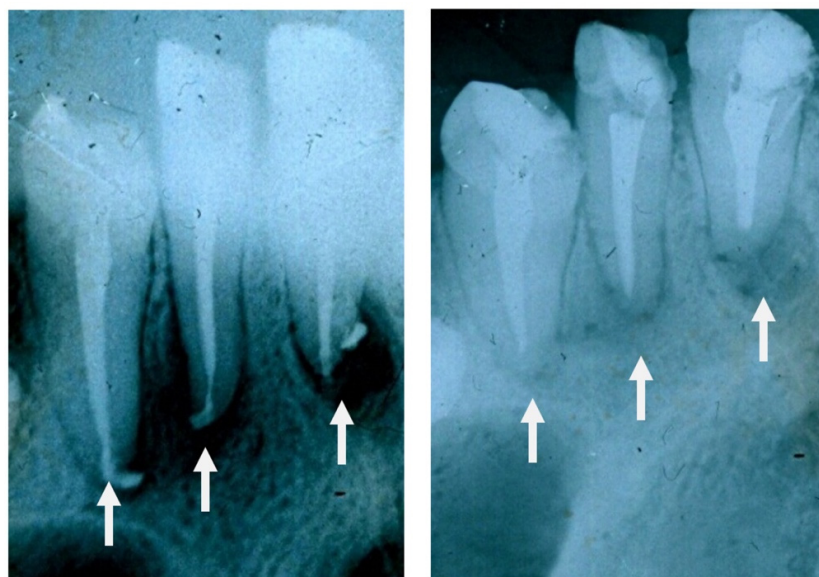


**Figure 12.** High-magnification radiographs of the patient before ((left) side) and after 2 months from operation ((right) side) showing that the lesions were filled up with trabeculae of new bone.

## 7. Towards the Future: 1d-Derived GC Dental Implants and Porous Scaffolds

### 7.1. GC Dental Implants

Dental implants rely on osteointegration through osteoinduction (whereby osteogenesis is induced) and osteoconduction, which involves the formation of hydroxyapatite [56–58]. The mechanical properties of natural tissues like the jawbone and dental hard tissue play a crucial role in the longevity of dental implants in the oral cavity [58,59]. After the placement of a prosthetic restoration, the dental implant receives the loads from the occlusal forces. When the elastic modulus and fracture toughness of the implant material align closely with those of the jawbone, the implant can effectively distribute the load to the adjacent bone, maintaining its density. However, if these properties differ significantly from those of the jawbone, then the dental implant is the only one that is loaded mechanically by the occlusal forces; as a result, the implant does not transfer the occlusal forces to the jawbone. This phenomenon is called stress shielding [60], whereby the osteocytes lose their main role (i.e., the preservation of the extracellular matrix), resulting in a reduction in the bone density of the jawbone, and eventually in the failure of the dental implant. The high elastic modulus of commonly-used dental implant materials like titanium alloys and zirconia (110 and 220 GPa, respectively) compared to the jawbone (7–30 GPa) and dentine (15–30 GPa) [31,61–64] is a common cause of implant failure and decreased bone density post-implantation. Bone grafts are utilized in various clinical scenarios when a patient's jawbone fails to meet the necessary criteria for optimal dental implant placement (specifically, due to insufficient bone quantity resulting from tooth loss) [31,62–64]. Initially, autogenous and allograft jawbone grafts were employed for their osteogenic and osteoinductive/osteoconductive properties, respectively. Subsequently, researchers redirected their focus towards synthetic materials (hydroxyapatite, tricalcium phosphates, bioactive glasses and GCs) to overcome the drawbacks associated with traditional grafts (such as patient discomfort, infection, complex surgical procedures, non-simultaneous absorption of the graft/new bone formation) and reduce costs [61–67].

According to Dimitriadis et al. [20,60], 1d-derived GCs display an excellent bioactive behaviour, yielding to spontaneous formation of hydroxyapatite on their surface after immersion in SBF at 37 °C. Besides having an adequate bioactivity, these GCs exhibited a well-sintered, dense microstructure embedding biocompatible crystalline phases that affected their mechanical properties (Table 4). These features, along with the attractive aesthetics (a white colour) [19,20], encourage further studies on such highly promising dental implant materials. More specifically, heat-treatment at 850 °C yielded GCs with



mechanical properties comparable to those of dentine (which is the biological tissue to be replaced by a dental implant) and the jawbone (which is the biological tissue put in direct contact with the material of a dental implant). Therefore, these appealing characteristics warrant further investigation regarding the suitability of 1d-based GCs in the production of dental implants.

The range of mechanical properties could be further modulated and finely tuned by combining the bioactive glass with biocompatible polymers, thus obtaining glass/polymer composites. These multiphase biomaterials allow combining the peculiar features of bioactive glasses, such as bioactivity and osteostimulatory properties, with the added values of polymers, including flexibility [68,69]. These composites show great promise in overcoming some traditional limits of bioactive glasses such as low fracture toughness, which is a particularly critical issue in glass-derived porous scaffolds [70].

### 7.2. Glass-Derived Porous Scaffolds

Biomaterials addressed to bone repair, including bioactive glasses or GCs, are often produced in the form of porous templates with architectural characteristics mimicking the trabecular structure of cancellous bone [71]. Following this “biomimicry-guided” criterion is thought to improve the regenerative properties of the implants, which are thus dictated not only by the inherent characteristics of the material (e.g., apatite-forming ability, biocompatibility with bone cells) but also by the porous geometry, allowing biofluids to flow in and out, cells to colonize the scaffold walls and blood vessel to grow in. Macroporous 1d-derived scaffolds have been recently fabricated for the first time using the sponge replica method [25]. Upon high-temperature thermal treatment at 800 °C for 3 h, the 1d glass particles underwent sinter-crystallization, leading to the consolidation of a scaffold structure and the concurrent development of diopside, fluorapatite and wollastonite, as expected from the material design. The sintered 1d-derived GC scaffolds exhibited a 3D pore-strut architecture and total porosity (68 vol.%) comparable to those of cancellous bone, while the compressive strength (29.7 MPa) and elastic modulus (1.4 GPa) were even superior to those of trabecular bone tissue (50–500 MPa), suggesting suitability for application in load-bearing sites. The scaffolds were also highly bioactive *in vitro* as demonstrated by the formation of a calcium phosphate layer after immersion in SBF for just 48 h. In an attempt to improve the scaffold reproducibility and the scalability of the whole fabrication process, early trials using additive manufacturing technologies to process 1d glass powders are currently ongoing in the context of a research collaboration among the authors of this review article.

## 8. Conclusions

Since its invention, 45S5 Bioglass<sup>®</sup> has been implanted in millions of human patients and is currently being marketed for various dental and orthopaedic applications. This has led to a considerable effort towards understanding the fundamentals that govern the physical, chemical and biological properties of bioactive glasses based on—or inspired by—45S5 glass. On the other hand, some limitations of the 45S5 composition—e.g., the high pH environment created by a high sodium content and poor sinterability—pushed scientists to develop new bioactive glass formulations. In this regard, bioactive glasses belonging to the CaO-MgO-SiO<sub>2</sub> ternary system as well as their relevant GC derivatives that feature low sodium oxide contents can indeed be used in bone repair as an alternative to the “gold standard” reference 45S5 Bioglass<sup>®</sup>. This was demonstrated through promising *in vitro* results on 1d glass that were corroborated by *in vivo* tests. The experimental data collected over the past 15 years supports the suitability of 1d glass in a variety of clinical applications for the repair of periodontal defects, ridge preservation and sinus augmentation. The full potential of bioactive glasses and GCs based on the CaO-MgO-SiO<sub>2</sub> ternary system, with special reference to the 1d composition, is still to be fully exploited and indeed deserves further investigation in the near future.

**Author Contributions:** Conceptualization, D.U.T. and F.B.; methodology, D.U.T., S.A., K.D., H.R.F., R.G. and F.B.; validation, D.U.T.; investigation, D.U.T., S.A., K.D., H.R.F., R.G. and F.B.; writing—original draft preparation, D.U.T. and F.B.; writing—review and editing, S.A., K.D., H.R.F. and R.G.; supervision, D.U.T. and F.B.; project administration, F.B.; funding acquisition, F.B. All authors have read and agreed to the published version of the manuscript.

**Funding:** This study was partially carried out within the project “Artificial Intelligence-based design of 3D PRINTed scaffolds for the repair of critical-sized BONE defects—I-PRINT-MY-BONE” funded by the European Union—Next Generation EU within the PRIN 2022 program (D.D. 104—02/02/2022 Ministero dell’Università e della Ricerca). This manuscript reflects only the authors’ views and opinions, and the Ministry cannot be considered responsible for them.

**Data Availability Statement:** No new data were created in this study, which is a review article. Original data can be found in the cited references.

**Acknowledgments:** D.T. thanks J.M.F. Ferreira from the University of Aveiro (Portugal) whose support, guidance and great expertise were instrumental in shaping the research direction.

**Conflicts of Interest:** The authors declare no conflicts of interest.

## References

1. Hench, L.L. The story of Bioglass. *J. Mater. Sci. Mater. Med.* **2006**, *17*, 967978. [[CrossRef](#)]
2. Wu, C.; Chang, J. Mesoporous bioactive glasses: Structure characteristics, drug/growth factor delivery and bone regeneration application. *Interface Focus* **2012**, *2*, 292–306. [[CrossRef](#)]
3. Moeini, A.; Hassanzadeh Chinijani, T.; Malek Khachatourian, A.; Fook, M.V.L.; Bairo, F.; Montazerian, M. A critical review of bioactive glasses and glass-ceramics in cancer therapy. *Int. J. Appl. Glass. Sci.* **2023**, *14*, 69–87. [[CrossRef](#)]
4. Miguez-Pacheco, V.; Greenspan, D.; Hench, L.; Boccaccini, A. Bioactive glasses in soft tissue repair. *Am. Ceram. Soc. Bull.* **2015**, *94*, 27–31.
5. Hench, L.L.; Greenspan, D. Interactions between bioactive glass and collagen: A review and new perspectives. *J. Aust. Ceram. Soc.* **2013**, *49*, 1–40.
6. Hench, L.L. Bioactive ceramics. *Ann. N. Y. Acad. Sci.* **1988**, *523*, 54–71. [[CrossRef](#)]
7. Roy, M.; Bandyopadhyay, A.; Bose, S. Ceramics in Bone Grafts and Coated Implants. In *Materials for Bone Disorders*, 1st ed.; Bandyopadhyay, A., Bose, S., Eds.; Elsevier: Philadelphia, PA, USA, 2017; pp. 265–314.
8. Bi, L.; Rahaman, M.N.; Day, D.E.; Brown, Z.; Samujh, C.; Liu, X.; Mohammadkhan, A.; Dusevich, V.; Eick, J.D.; Bonewald, L.F. Effect of bioactive borate glass microstructure on bone regeneration, angiogenesis, and hydroxyapatite conversion in a rat calvarial defect model. *Acta Biomater.* **2013**, *9*, 8015–8026. [[CrossRef](#)]
9. Abou Neel, E.A.; Pickup, D.M.; Valappil, S.P.; Newport, R.J.; Knowles, J.C. Bioactive functional materials: A perspective on phosphate-based glasses. *J. Mater. Chem.* **2009**, *19*, 690–701. [[CrossRef](#)]
10. McEntire, B.; Bal, B.S.; Rahaman, M.; Chevalier, J.; Pezzotti, G. Ceramics and ceramic coatings in orthopaedics. *J. Eur. Ceram. Soc.* **2015**, *35*, 4327–4369. [[CrossRef](#)]
11. Balasubramanian, S.; Gurumurthy, B.; Balasubramanian, A. Biomedical applications of ceramic nanomaterials: A review. *Int. J. Pharma Sci. Res.* **2017**, *8*, 4950–4959.
12. Shanmugam, K.; Sahadevan, R. Bioceramics—An Introductory Overview. In *Fundamental Biomaterials: Ceramics*, 1st ed.; Thomas, S., Balakrishnan, P., Sreekala, M.S., Eds.; Elsevier Ltd.: Philadelphia, PA, USA, 2018; pp. 1–46.
13. Montazerian, M.; Zanotto, E.D. History and trends of bioactive glass-ceramics. *J. Biomed. Mater. Res. A* **2016**, *104*, 1231–1249. [[CrossRef](#)] [[PubMed](#)]
14. Blayney, A.W.; Bebear, J.P.; Williams, K.R.; Portmann, M. Ceravital in ossiculoplasty: Experimental studies and early clinical results. *Am. J. Otol.* **1986**, *100*, 1359–1366. [[CrossRef](#)] [[PubMed](#)]
15. Nonami, T.; Tsutsumi, S. Study of diopside ceramics for biomaterials. *J. Mater. Sci. Mater. Med.* **1999**, *10*, 475–479. [[CrossRef](#)] [[PubMed](#)]
16. Salinas, A.J.; Vallet-Regí, M. Bioactive ceramics: From bone grafts to tissue engineering. *RSC Adv.* **2013**, *3*, 11116–11131. [[CrossRef](#)]
17. Peitl, O.; LaTorre, G.P.; Hench, L.L. Effect of crystallization on apatite layer formation of bioactive glass 45S5. *J. Biomed. Mater. Res.* **1996**, *30*, 509–514.
18. Kansal, I.; Tulyaganov, D.U.; Goel, A.; Pascual, M.J.; Ferreira, J.M.F. Structural analysis and thermal behavior of diopside fluorapatite wollastonite based glasses and glass ceramics. *Acta Biomater.* **2010**, *6*, 4380–4388. [[CrossRef](#)] [[PubMed](#)]
19. Dimitriadis, K.; Vasilopoulos, K.C.; Vaimakis, T.C.; Karakassides, M.A.; Tulyaganov, D.U.; Agathopoulos, S. Synthesis of glass ceramics in the Na<sub>2</sub>O/K<sub>2</sub>O-CaO-MgO-SiO<sub>2</sub>-P<sub>2</sub>O<sub>5</sub>-CaF<sub>2</sub> system as candidate materials for dental applications. *Int. J. Appl. Ceram. Technol.* **2020**, *17*, 2025–2035. [[CrossRef](#)]
20. Dimitriadis, K.; Moschovas, D.; Tulyaganov, D.U.; Agathopoulos, S. Development of novel bioactive glass ceramics in the Na<sub>2</sub>O/K<sub>2</sub>O-CaO-MgO-SiO<sub>2</sub>-P<sub>2</sub>O<sub>5</sub>-CaF<sub>2</sub> system. *J. Non-Cryst. Solids* **2020**, *533*, 119936. [[CrossRef](#)]

21. Tulyaganov, D.U.; Agathopoulos, S.; Ventura, J.M.G.; Karakassides, M.A.; Fabrichnaya, O.; Ferreira, J.M.F. Synthesis of glass-ceramics in the CaO–MgO–SiO<sub>2</sub> system with B<sub>2</sub>O<sub>3</sub>, P<sub>2</sub>O<sub>5</sub>, Na<sub>2</sub>O and CaF<sub>2</sub> additives. *J. Eur. Ceram. Soc.* **2006**, *26*, 1463–1471. [[CrossRef](#)]
22. Tulyaganov, D.U.; Agathopoulos, S.; Valerio, P.; Balamurugan, A.; Saranti, A.; Karakassides, M.A.; Ferreira, J.M.F. Synthesis, bioactivity and preliminary biocompatibility studies of glasses in the system CaO–MgO–SiO<sub>2</sub>–Na<sub>2</sub>O–P<sub>2</sub>O<sub>5</sub>–CaF<sub>2</sub>. *J. Mater. Sci. Mater. Med.* **2011**, *22*, 217–227. [[CrossRef](#)]
23. Schmitz, S.I.; Widholz, B.; Essers, C.; Becker, M.; Tulyaganov, D.U.; Moghaddam, A.; Gonzalo de Juan, I.; Westhauser, F. Superior biocompatibility and comparable osteoinductive properties: Sodium-reduced fluoride-containing bioactive glass belonging to the CaO–MgO–SiO<sub>2</sub> system as a promising alternative to 45S5 bioactive glass. *Bioact. Mater.* **2020**, *5*, 55–65. [[CrossRef](#)] [[PubMed](#)]
24. Tulyaganov, D.U.; Akbarov, A.; Zyyadullaeva, N.; Khabilov, B.; Bains, F. Injectable bioactive glass-based pastes for potential use in bone tissue repair. *Biomed. Glas.* **2020**, *6*, 23–33. [[CrossRef](#)]
25. Bains, F.; Tulyaganov, D.U.; Kahharov, Z.; Rahdar, A.; Vernè, E. Foam-Replicated Diopside/Fluorapatite/Wollastonite-Based Glass–Ceramic Scaffolds. *Ceramics* **2022**, *5*, 120–130. [[CrossRef](#)]
26. Tulyaganov, D.U.; Makhkamov, M.E.; Urazbaev, A.; Goel, A.; Ferreira, J.M.F. Synthesis, processing and characterization of a bioactive glass composition for bone regeneration. *Ceram. Int.* **2013**, *39*, 2519–2526. [[CrossRef](#)]
27. Boccaccini, A.R. Machinability and brittleness of glass-ceramics. *J. Mater. Process Technol.* **1997**, *65*, 302–304. [[CrossRef](#)]
28. Dimitriadis, K.; Tulyaganov, D.U.; Agathopoulos, S. Production of Bioactive Glass–Ceramics for Dental Application through Devitrification of Glasses in the Na<sub>2</sub>O/K<sub>2</sub>O–CaO–MgO–SiO<sub>2</sub>–P<sub>2</sub>O<sub>5</sub>–CaF<sub>2</sub> System. In *Bioactive Glasses and Glass–Ceramics: Fundamentals, Applications, and Advances*; Bains, F., Kargozar, S., Eds.; John Wiley and Sons Ltd.: Hoboken, NJ, USA, 2022; pp. 431–457.
29. Kapoor, S.; Goel, A.; Filipa, A.; Pascual, M.J.; Lee, H.; Kim, H.; Ferreira, J.M.F. Influence of ZnO/MgO substitution on sintering, crystallisation, and bio-activity of alkali-free glass-ceramics. *Mater. Sci. Eng. C* **2015**, *53*, 252–261. [[CrossRef](#)]
30. Soares, V.O.; Daguano, J.K.M.B.; Lombello, C.B.; Bianchin, O.S.; Gonçalves, L.M.G.; Zanotto, E.D. New sintered wollastonite glass-ceramic for biomedical applications. *Ceram. Int.* **2018**, *44*, 20019–20027. [[CrossRef](#)]
31. Saadaldin, S.A.; Rizkalla, A.S. Synthesis and characterization of wollastonite glassceramics for dental implant applications. *Dent. Mater.* **2014**, *30*, 364–371. [[CrossRef](#)]
32. Saadaldin, S.A.; Dixon, S.J.; Rizkalla, A.S. Bioactivity and biocompatibility of a novel wollastonite glass-ceramic biomaterial. *J. Biomater. Tissue Eng.* **2014**, *4*, 939–946. [[CrossRef](#)]
33. Garcia, E.; Miranzo, P.; Sainz, M.A. Thermally sprayed wollastonite and wollastonite-diopside compositions as new modulated bioactive coatings for metal implants. *Ceram. Int.* **2018**, *44*, 12896–12904. [[CrossRef](#)]
34. Dorozhkin, S.V. Calcium orthophosphates as bioceramics: State of the art. *J. Funct. Mater.* **2010**, *1*, 22–107. [[CrossRef](#)]
35. Ramadoss, R.; Padmanaban, R.; Subramanian, B. Role of bioglass in enamel remineralization: Existing strategies and future prospects—A narrative review. *J. Biomed. Mater. Res. B Appl. Biomater.* **2022**, *110*, 45–66. [[CrossRef](#)] [[PubMed](#)]
36. Wiglusz, K.; Dobrzynski, M.; Gutbier, M.; Wiglusz, R.J. Nanofluorapatite Hydrogels in the treatment of Dentin Hypersensitivity: A study of physiochemical Properties and Fluoride Release. *Gels* **2023**, *9*, 271–287. [[CrossRef](#)]
37. Zenebe, C.G. A Review on the Role of Wollastonite Biomaterial in Bone Tissue Engineering. *BioMed Res. Int.* **2022**, *2022*, 996530. [[CrossRef](#)]
38. Tulyaganov, D.U.; Dimitriadis, K.; Agathopoulos, S.; Bains, F.; Fernandes, H.R. Wollastonite-containing glass-ceramics from the CaO–Al<sub>2</sub>O<sub>3</sub>–SiO<sub>2</sub> and CaO–MgO–SiO<sub>2</sub> ternary systems. *Open Ceram.* **2024**, *17*, 100507. [[CrossRef](#)]
39. Kokubo, T.; Shigematsu, M.; Nagashima, Y.; Tashiro, M.; Nakamura, T.; Yamamuro, T.; Higashi, S. Apatite-and wollastonite-containing glass-ceramics for prosthetic application. *Bull. Inst. Chem. Res. Kyoto Univ.* **1982**, *60*, 260–268.
40. Hench, L.L.; Splinter, R.J.; Allen, W.C.; Greenlee, T.K. Bonding mechanisms at the interface of ceramic prosthetic materials. *J. Biomed. Mater. Res.* **1971**, *5*, 117–141. [[CrossRef](#)]
41. Vichaphund, S.; Kitiwan, M.; Atong, D.; Thavorniti, P. Microwave synthesis of wollastonite powder from eggshells. *J. Eur. Ceram. Soc.* **2011**, *31*, 2435–2440. [[CrossRef](#)]
42. He, Z.; Shen, A.; Lyu, Z.; Li, Y.; Wu, H.; Wang, W. Effect of wollastonite microfibers as cement replacement on the properties of cementitious composites: A review. *Constr. Build. Mater.* **2020**, *261*, 119920. [[CrossRef](#)]
43. “Chrome Diopside”, Chemistry Views. 22 May 2014. Available online: [https://www.chemistryviews.org/details/ezone/6047511/Chrome\\_Diopside/#:~:text=Diopside%20has%20the%20composition%20CaMgSi,the%20crystals%20are%20often%20twinned](https://www.chemistryviews.org/details/ezone/6047511/Chrome_Diopside/#:~:text=Diopside%20has%20the%20composition%20CaMgSi,the%20crystals%20are%20often%20twinned) (accessed on 1 November 2023).
44. “A Surprisingly Important Structure-Diopside”, Crystallography365. 23 August 2014. Available online: <https://crystallography365.wordpress.com/2014/08/23/a-surprisingly-important-structure-diopside/> (accessed on 1 November 2023).
45. Wang, G.C.; Lu, Z.F.; Zreiqat, H. Bioceramics for Skeletal Bone Regeneration. In *Bone Substitute Biomaterials*, 1st ed.; Mallick, K., Ed.; Woodhead Publishing: Cambridge, UK, 2014; pp. 180–186.
46. Dietrich, E.; Oudadesse, H.; Lucas Girot, A.; Le Gal, Y.; Jeanne, S.; Cathelineau, G. Effects of Mg and Zn on the surface of doped melt derived glass for biomaterials applications. *Appl. Surf. Sci.* **2008**, *255*, 391–395. [[CrossRef](#)]
47. Tilocca, A. Structural models of bioactive glasses from molecular dynamics simulations. *Proc. R Soc. A* **2009**, *465*, 1003–1027. [[CrossRef](#)]

48. Brauer, D.S.; Karpulthina, N.; O'Donnell, M.D.; Law, R.V.; Hill, R.G. Fluoride-containing bioactive glasses: Effect of glass design and structure on degradation, pH and apatite formation in simulated body fluid. *Acta Biomater.* **2010**, *6*, 3275–3282. [[CrossRef](#)] [[PubMed](#)]
49. Mozafari, M.; Banijamali, S.; Baino, F.; Kargozar, S.; Hill, R.G. Calcium carbonate: Adored and ignored in bioactivity assessment. *Acta Biomater.* **2019**, *91*, 35–47. [[CrossRef](#)] [[PubMed](#)]
50. Khoshniat, S.; Bourguine, A.; Julien, M.; Petit, M.; Pilet, P.; Rouillon, T.; Masson, M.; Gatiús, M.; Weiss, P.; Guicheux, J.; et al. Phosphate-dependent stimulation of MGP and OPN expression in osteoblasts via the ERK1/2 pathway is modulated by calcium. *Bone* **2011**, *48*, 894–902. [[CrossRef](#)] [[PubMed](#)]
51. Reffitt, D.M.; Ogston, N.; Jugdaohsingh, R.; Cheung, H.F.; Evans, B.A.; Thompson, R.P.; Powell, J.J.; Hampson, G.N. Orthosilicic acid stimulates collagen type 1 synthesis and osteoblastic differentiation in human osteoblast-like cells in vitro. *Bone* **2003**, *32*, 127–135. [[CrossRef](#)]
52. Zheng, J.; Mao, X.; Ling, J.; Chen, C.; Zhang, W. Role of magnesium transporter subtype 1 (MagT1) in the osteogenic differentiation of rat bone marrow stem cells. *Biol. Trace Elem. Res.* **2016**, *171*, 131–137. [[CrossRef](#)] [[PubMed](#)]
53. Hench, L.L. Genetic design of bioactive glasses. *J. Eur. Ceram. Soc.* **2009**, *29*, 1257–1265. [[CrossRef](#)]
54. Gonzalo-Juan, I.; Xie, F.; Becker, M.; Tulyaganov, D.U.; Fischer, A.; Riedel, R. Synthesis of silver modified bioactive glassy materials with antibacterial properties via facile and low-temperature route. *Materials* **2020**, *13*, 5115. [[CrossRef](#)] [[PubMed](#)]
55. Gonzalo-Juan, I.; Tulyaganov, D.U.; Balan, C.; Linser, R.; Ferreira, J.M.F.; Riedel, R.; Ionescu, E. Tailoring the viscoelastic properties of injectable biocomposites: A spectroscopic assessment of the interactions between organic carriers and bioglass particles. *Mater. Des.* **2016**, *97*, 45–50. [[CrossRef](#)]
56. Jones, J.R.; Brauer, D.S.; Hupa, L.; Greenspan, D.C. Bioglass and bioactive glasses and their impact on healthcare. *Int. J. Appl. Glass Sci.* **2016**, *7*, 423–434. [[CrossRef](#)]
57. Fernandes, H.R.; Gaddam, A.; Rebelo, A.; Brazete, D.; Stan, G.E.; Ferreira, J.M.F. Bioactive glasses and glass-ceramics for healthcare applications in bone regeneration and tissue engineering. *Materials* **2018**, *11*, 2530. [[CrossRef](#)]
58. Albrektsson, T.; Johansson, C. Osteoinduction, osteoconduction and osseointegration. *Eur. Spine J.* **2001**, *10*, S96–S101.
59. Lakatos, É.; Magyar, L.; Bojtár, I. Material properties of the mandibular trabecular bone. *J. Med. Eng.* **2014**, *2014*, 470539. [[CrossRef](#)]
60. Dimitriadis, K.; Tulyaganov, D.U.; Agathopoulos, S. Development of novel alumina-containing bioactive glass-ceramics in the CaO-MgO-SiO<sub>2</sub> system as possible candidates for dental implant applications. *J. Eur. Ceram. Soc.* **2021**, *41*, 929–940. [[CrossRef](#)]
61. Montazerian, M.; Zanutto, E.D. Bioactive and inert dental glass-ceramics. *Biomed. Mater. Res. A* **2017**, *105*, 619–639. [[CrossRef](#)] [[PubMed](#)]
62. Saadaldin, S.A.; Dixon, S.J.; Costa, D.O.; Rizkalla, A.S. Synthesis of bioactive and machinable miserite glass-ceramics for dental implant applications. *Dent. Mater.* **2013**, *29*, 645–655. [[CrossRef](#)] [[PubMed](#)]
63. Fillingham, Y.; Jacobs, J. Bone grafts and their substitutes. *Bone Jt. J.* **2016**, *98-B*, 6–9. [[CrossRef](#)]
64. Laurencin, C.; Khan, Y.; El-Amin, S.F. Bone graft substitutes. *Expert. Rev. Med. Devices* **2006**, *3*, 49–57. [[CrossRef](#)] [[PubMed](#)]
65. Kumar, P.; Vinitha, B.; Fathima, G. Bone grafts in dentistry. *J. Pharm. Bioallied. Sci.* **2013**, *5*, S125–S127. [[CrossRef](#)]
66. Chen, Q.Z.; Thompson, I.D.; Boccaccini, A.R. 45S5 Bioglass-derived glass-ceramic scaffolds for bone tissue engineering. *Biomaterials* **2006**, *27*, 2414–2425. [[CrossRef](#)] [[PubMed](#)]
67. Fu, L.; Engqvist, H.; Xia, W. Glass-ceramics in dentistry: A review. *Materials*. **2020**, *13*, 1049. [[CrossRef](#)]
68. Rezwan, K.; Chen, Q.Z.; Blaker, J.J.; Boccaccini, A.R. Biodegradable and bioactive porous polymer/inorganic composite scaffolds for bone tissue engineering. *Biomaterials* **2006**, *27*, 3413–3431. [[CrossRef](#)] [[PubMed](#)]
69. Mohamad Yunos, D.; Bretcanu, O.; Boccaccini, A.R. Polymer-bioceramic composites for tissue engineering scaffolds. *J. Mater. Sci.* **2008**, *43*, 4433–4442. [[CrossRef](#)]
70. Rehorek, L.; Chlup, Z.; Meng, D.; Yunos, D.M.; Boccaccini, A.R.; Dlouhy, I. Response of 45S5 bioglass<sup>®</sup> foams to tensile loading. *Ceram. Int.* **2013**, *39*, 8015–8020. [[CrossRef](#)]
71. Baino, F.; Fiume, E.; Barberi, J.; Kargozar, S.; Marchi, J.; Massera, J.; Verné, E. Processing methods for making porous bioactive glass-based scaffolds—A state-of-the-art review. *Int. J. Appl. Ceram. Technol.* **2019**, *16*, 1762–1796. [[CrossRef](#)]

**Disclaimer/Publisher's Note:** The statements, opinions and data contained in all publications are solely those of the individual author(s) and contributor(s) and not of MDPI and/or the editor(s). MDPI and/or the editor(s) disclaim responsibility for any injury to people or property resulting from any ideas, methods, instructions or products referred to in the content.